R. Kirchner, R. Hoekstra, N. Chidambaram, H. Schift

Depth-profiling of vertical material contrast after VUV exposure for contact-free polishing of 3D polymer micro-optics

Erstveröffentlichung in / First published in:

33rd European Mask and Lithography Conference. Dresden, 2017. Bellingham: SPIE, Vol. 10428 *[Zugriff am: 02.05.2019]*.

DOI: https://doi.org/10.1117/12.2279712

Depth-profiling of vertical material contrast after VUV exposure for contact-free polishing of 3D polymer micro-optics

R. Kirchner, R. Hoekstra, N. Chidambaram, H. Schift

R. Kirchner, R. Hoekstra, N. Chidambaram, H. Schift, "Depth-profiling of vertical material contrast after VUV exposure for contact-free polishing of 3D polymer micro-optics
," Proc. SPIE 10446, 33rd European Mask and Lithography Conference, 1044613 (28 September 2017); doi: 10.1117/12.2279712

SPIE.

Event: 33rd European Mask and Lithography Conference, 2017, Dresden, Germany

Depth-profiling of vertical material contrast after VUV exposure for contact-free polishing of 3D polymer micro-optics

R. Kirchner*[a], R. Hoekstra[b], N. Chidambaram[b], and H. Schift[b]
[a] Technische Universität Dresden, Institute of Semiconductors and Microsystems, 01062 Dresden, Germany
[b] Paul Scherrer Institute, Laboratory for Micro- and Nanotechnology, 5232 Villigen PSI, Switzerland

ABSTRACT

We characterize the impact of high-energy, 172 nm vacuum ultraviolet photons on the molecular weight and the glass transition temperature of poly(methyl methacrylate). We found that the molecular weight is reduced strongly on the surface of the exposed samples with a continuous transition towards the unexposed bulk material being located below the modified region. The glass transition temperature was found to be significantly lowered in the exposed region to well below 50°C compared to that of the 122°C of the bulk region. We could use this material contrast to selectively reflow the top surface of the exposed samples only. This allowed us to create ultra-smooth micro-optical structures by post-processing without influencing the overall geometry that is required for the optical functionality.

Keywords: glass transition, molecular weight, chain scission, thermal expansion, reflow, multi-photon lithography

1. INTRODUCTION

Creating material contrast is the basic principle of lithography since the fabrication of integrated electronic circuits. To transfer the image of a mask into a resist material, an exposure or writing process creates a latent image in terms of different solubility of the resist regions due to modification of the resist by high-energy radiation. This radiation comprises in most cases photons, electrons or ions. To create a topography contrast, this latent image is transformed into a physical topography during the development process by chemicals that selectively remove parts of the latent image in the resist. For example, for a positive tone resist the solubility in the developer is enhanced and the exposed regions are dissolved and removed. This enhanced solubility can be among others due to a reduced molecular weight of a linear polymer in a solvent. A well-known example is poly(methyl methacrylate) (PMMA) often used as positive tone electron beam lithography (EBL) resist. Upon exposure with high-energy electrons, the molecular weight M_w is significantly reduced due to electron induced chain scission [1]. As shown in several publications, the reduced M_w in PMMA leads to a reduced glass transition temperature T_g especially when it falls below a certain critical molecular weight [2-4]. By defining a contrast in T_g, a much broader diversity of micro-lenses can be for example created compared to the classical reflow process [5,6]. A lateral contrast of T_g allows to create an asymmetric polymer reflow profile [3,7,8]. In contrast, a vertical T_g contrast as used in this work enables to selectively initiate polymer relocation on the surface of a thick polymer film or structure while the bulk of this polymer structure will remain unaffected [4]. This can be for example used to create ultra-smooth micro optics [4,9-11].

The glass transition region is a special region because many physical properties are significantly different below and above this region while a gradual change of these properties take place within this region. One such a particular property is the thermal expansion that can be described by the linear coefficient of thermal expansion (CTE). The CTE as well as the refractive index are significantly different below and above the T_g region due to the free volume increase during glass transition. The thickness and, thus, also the CTE is well accessible using optical probes such as ellipsometry [12] or white light reflectometry as used in this work.

We characterize the exposure impact on the M_w based on scanning electron micrographs and on the T_g based on measurement of the thermal expansion. We further demonstrate the reduction of the surface roughness based on the confined modification of the T_g of the surface of a micro-optical diffuser and a micro-prism array.

* robert.kirchner@tu-dresden.de; phone +49 (0) 351 463 39897; https://tu-dresden.de/ing/elektrotechnik/ihm

33rd European Mask and Lithography Conference, edited by Uwe F.W. Behringer, Jo Finders, Proc. of SPIE Vol. 10446, 1044613 · © 2017 SPIE
CCC code: 0277-786X/17/$18 · doi: 10.1117/12.2279712

2. MATERIALS AND METHODS

2.1 172 nm VUV exposure

The surface of PMMA samples was exposed by 172 nm vacuum ultraviolet (VUV) photons using a commercial lab setup (EX-mini, Hamamatsu Photonics K.K.) under ambient conditions with a short distance of 3 mm and 10 mm to the lamp housing to ensure a high enough photon impact (Fig. 1). The nominal VUV output power is about 50 mW/cm^2. The photon energy for the used distance was about 16.3 mW/cm^2 and 5.5 mW/cm^2 based on a calibration curve for 3 mm and 10 mm, respectively. Typical exposure times were up to 60 s. The PMMA samples were prepared by spin-coating of PMMA120k (micro resist technology GmbH) and post-apply baked at 140°C for 2 min. Subsequently, the samples were exposed and immediately characterized by the methods mentioned below.

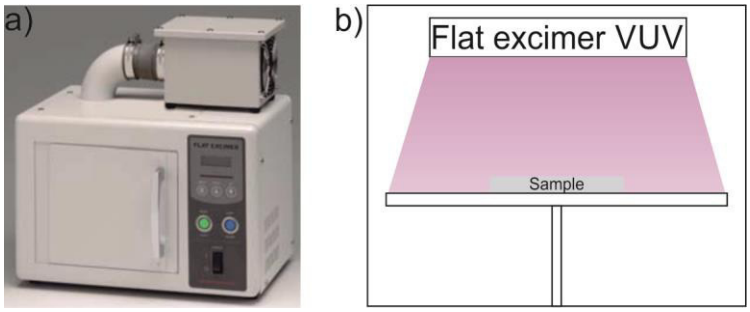

Figure. 1: a) Photograph and b) schematic of the exposure setup with a 172 nm wavelength, flat excimer lamp.

2.2 SEM cross sections

The mechanical properties of PMMA strongly depend on the M_w. A low M_w PMMA breaks much less brittle compared to a high M_w PMMA. Figure 2 gives an example for a selectively EBL exposed and developed sample after manual, crystal oriented cleaving of the PMMA film being located on top of a silicon sample. After exposure with different doses and before cleaving, the samples were developed for a given time. Due to the different M_w, the development rates were also differing in the exposed sections and led to a staircase profile [3]. More interesting is the effect on the M_w. While the unexposed part (D_0) has a rough and granular cleaving facet, this granularity decreases with increasing electron beam dose (D_1-D_3) due to a less brittle behavior of the PMMA during cleaving. The M_w regions are clearly separated in lateral direction due to the complete penetration and minimum forward scattering of the electrons in the resist due to the used 100 keV EBL system (Vistec B.V., EBPG 5000 Plus).

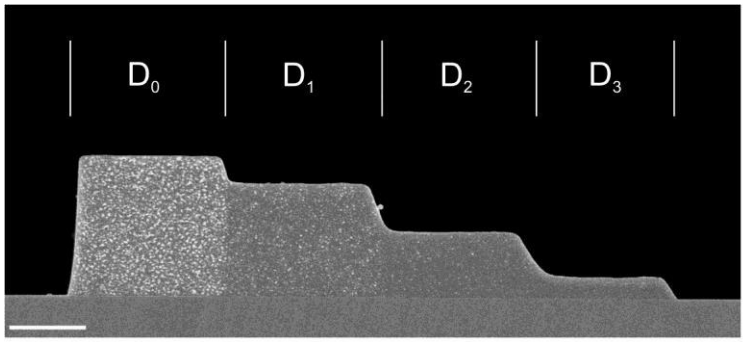

Dose D_x (μC/cm2)	M_{wx} (kg/mol)	T_{gx} (°C)
0	91.2	122
120	29.2	106
200	18.0	101
270	13.0	97

Figure 2. Profile of an electron beam exposed sample with increasing dose from the first step D_0 until the last step D_3 (D_0 = 0 μC/cm^2, D_1 = 120 μC/cm^2, D_2 = 200 μC/cm^2, D_3 = 270 μC/cm^2). Outside the steps, a larger dose (dose-to-clear) was applied. The granularity of the cleaved facets is governed by the M_w of the respective region. The tabulated data is based on Ref. [3]. (Scale bar 1 μm)

2.3 Development rates

The development rate of exposed PMMA depends on the exposure dose. The higher the dose is, the lower is the M_w and the faster is the PMMA removed in a given solvent. We used the development rates for the EBL exposed PMMA120k and compared it to the development rates of the VUV exposed PMMA120k. By correlating the known T_g and the devel-

opment rates for EBL exposed samples, a first rough estimation of the T_g profile of the VUV exposed samples became possible. To measure the VUV development rates, large areas were masked by a metal shadow mask and iteratively developed for 2 s in the EBL developer methyl isobutyl ketone (MIBK) and subsequently rinsed in isopropyl alcohol (IPA) to stop the development process. The depth of the developed regions was measured by stylus profilometry (Dektak 8, Veeco Inc.) after each development step. The development rates were calculated as the removed thickness per time unit.

2.4 Linear thermoplastic expansion

To determine the linear CTE, VUV flood exposed samples were placed on a resistive heating strip and isolated against heating of the surrounding measurement setup being placed in an optical microscope. The film thickness was measured continuously using a white light reflectometry film thickness probe (FTP, Sentech Gmbh) with the microscopes 10x objective (Fig. 3a). Synchronized to the film thickness, the surface temperature of the PMMA120k sample was measured using a K-type thermocouple. The surface was continuously kept in focus for the complete measurement cycle by manual control. To minimize the effect on the sample, a yellow filter was applied to the beam path. The sample was slowly heated to a temperature above its expected T_g. For reasons of stability and accuracy, the film thickness was measured during the subsequent cooling of the samples back to room temperature. It was found that for excessively exposed samples, the film thickness continuously decreased when the temperature was kept constant for a too long time above T_g.

Due to the exponential absorption of the VUV photons, a similar exponential increase of the M_w from the surface down to the bulk can be expected. The lowest M_w chains on the surface are so small, that they become volatile and leave the sample surface during the exposure. This becomes visible by a reduced film thickness before and after exposure and the main reason for film thickness reduction and instabilities during the measurement process. This is also the limitation of the used measurement system: very low T_g values of the most upper material cannot be captured as this material evaporates immediately during the measurement. The remaining material has also no homogenous CTE as this CTE strongly depends on the T_g and thus the M_w depth profile. The exposed material can be imagined as a stack of films with a different CTE for each film and an infinitely small thickness per layer. In conclusion, the FTP measurements capture all CTEs of this material stack in an integrative manner. In consequence, one can extract the film thickness and the CTE change versus the temperature (Fig. 3b).

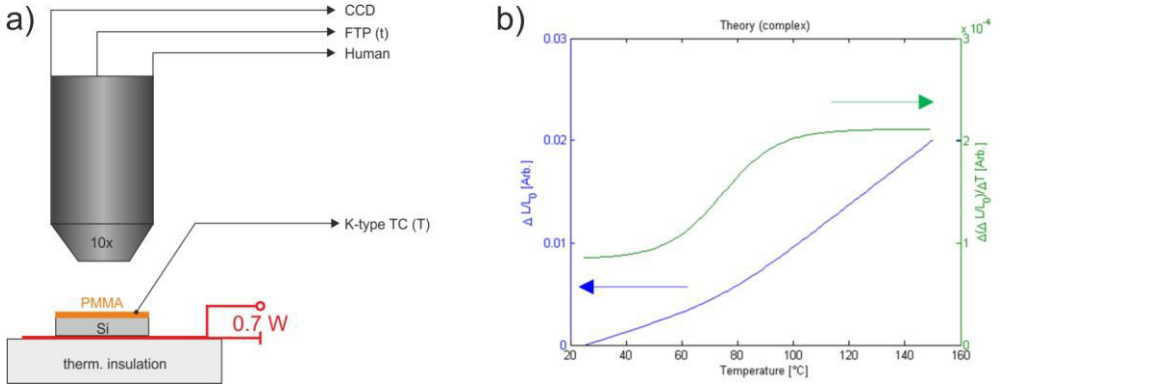

Figure 3. a) Measurement setup and b) exemplary graph of the relative film thickness increase and the first derivative of this versus the temperature defined as CTE. The complex theoretical film used here for visualization has a central T_g of 75°C and a width of the transition region of 40°C.

For simplicity, the refractive index was assumed to be constant over temperature which is the reason for a certain but acceptable inaccuracy of the measured values and part of ongoing process improvement.

2.5 Surface confined reflow and device fabrication

Optical diffuser structures and micro-prism reflectors were fabricated by direct laser writing using multi-photon lithography (MPL) and the obtained patterns were replicated from the MPL resist into the PMMA120k by nanoimprint lithography using elastomeric molds and hot embossing [4,11,13]. The negative tone MPL resist could not be treated in a similar way as describe here and thus required the pattern transfer into PMMA. This made the optical structures accessible for polymer reflow. The VUV exposed samples were globally heated on hotplate using a top-heater setup to additionally enhance the viscosity gradient from top to bottom of the structure due to the temperature gradient generated with the top-heater setup [11].

3. RESULTS AND DISCUSSION

3.1 Profile of SEM cross sections

SEM cross sections indicated only a mininmal removal of about 20 nm PMMA120k within 30 s of exposure in a distance of 3 mm to the lamp housing. For the intended smoothenign of micro-optics this has only a neglectabel influence on the device performance. The avarage thickness of the visible film modification was about 298±11 nm for different film thicknesses between 437 nm and 3994 nm (Fig. 4). This confirms an expected, constant modification thickness independent of the film thickness itself due to the exponential attanuation of the VUV photons starting from the top of the film. This exponential intensity decay is also visible in Figure 4 comparing the films ranging from the thickest (Fig. 4b) down to the thinnest film (Fig. 4e). The cleaving itself generates, in dependence of the M_w, additional facet features beign mostly located close to the substrate. However, comparing the less effected upper part of each thickness shows very similar features among all thciknesses: a completely smooth facet on top with a continous transition towards more granular and finally very rough facet well below the surface. This top 298 nm are, hence, most affected by the VUV photons. However, below this region there is evidence from this cross sections, that the modification is ranging more than 1 µm deep but has probably no significant effect on the T_g in this depth compared to the top 298 nm.

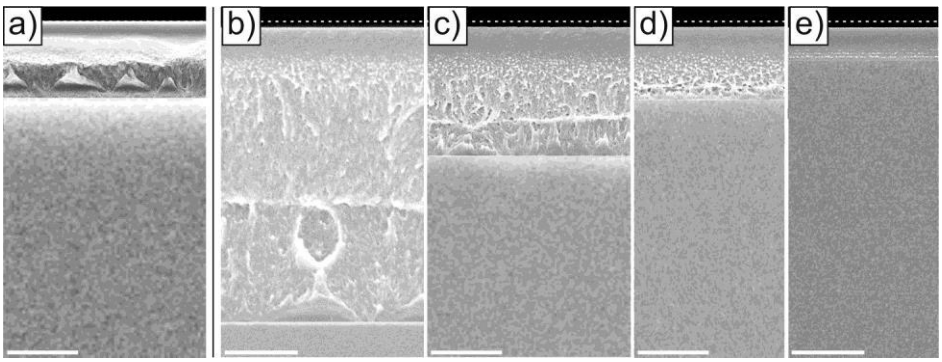

Figure 4. Comparison of a) unexposed PMMA120k with different exposed films (about 16.3 mW/cm^2 for 30 s) being b) 3994 nm thick, c) 1737 nm thick, d) 984 nm thick and e) 437 nm thick. The dashed line indicates the surface before exposure. (Scale bar 1 µm)

3.2 Development rates

In dependence of the exposure dose ranging from 98 mJ/cm^2 up to 488 mJ/cm^2, the development rates strongly increased and exceeded by far the rates found for the 100 keV electron beam exposed samples (Fig. 5). This is in agreement with literature findings that photons of about 190 nm wavelength are much more efficient in chain scission compared to 25 keV and thus even more pronounced compared to 100 keV electrons [14]. It is well known, that a higher acceleration voltage in EBL leads to a reduced sensitivity for the same resist material. While for low VUV doses of about 100 mJ/cm^2, the T_g was well in the range of the EBL samples and did not exceed 90°C in the most upper PMMA region (Fig. 5a), doses above 100 mJ/cm^2 resulted in a much more pronounce T_g reduction (Fig. 5b). For the smaller doses an almost linear decay of the T_g is visible reaching the bulk behavior already about 200 nm from the top surface. While this is not sufficient to efficiently reduce roughness in the 100 nm range without influencing the bulk material, the higher doses create a more useful, significant contrast between the top film and the bulk. The T_g drops almost exponentially with a quite sharp transition about 300 nm to 400 nm from the surface. Using even more dose will enhance this contrast and also increase the modified film thickness but ultimately will lead to a strong ablation or etching of the film surface. This ablation limit defines the maximum dose that can be used for material modification without significant shape deterioration of an optical device.

Regarding the T_g values determined for EBL [3] (cf. Fig. 2), the generally much larger development rates suggest a much lower T_g for the VUV exposed samples compared to the EBL samples. A rough estimation based on the extrapolation of the EBL sample T_g values using the EBL development rates and a VUV exposure with known development rate (Fig. 6) places the VUV T_g in the range of 30°C to 40°C in the top surface for the high dose VUV exposure. An improved T_g measurement is expected from CTE setup.

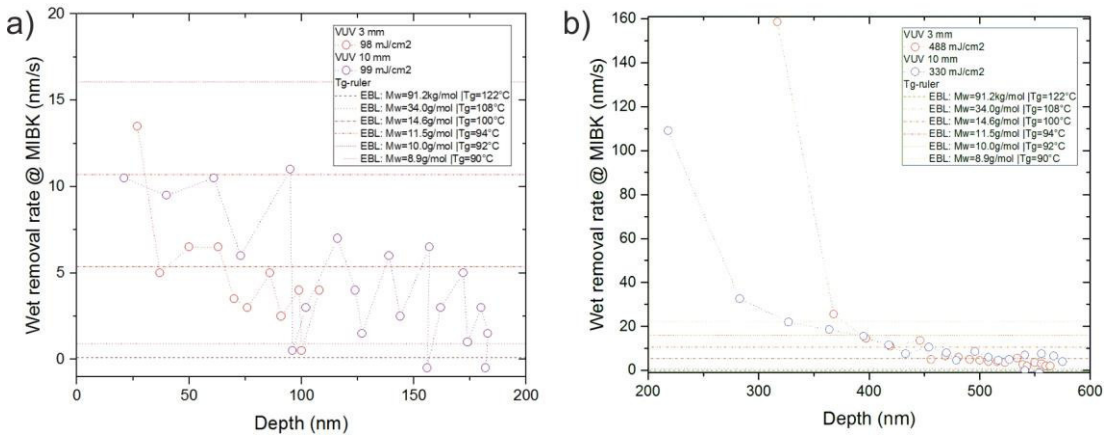

Figure 5. Plot of the solvent removal rate as depth profile measured from discrete points in time during the development process for a) low and b) much high VUV doses.

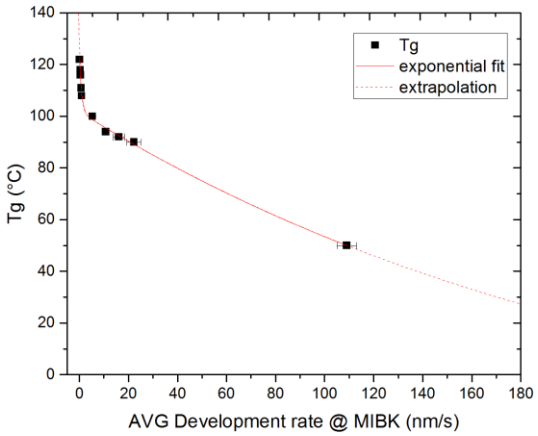

Figure 6. Consolidated plot of EBL obtained development rates (< 30 nm/s) and a VUV exposure with an averaged T_g estimation (109 nm/s) using a double exponential decay to fit and to extrapolate the data for a rough T_g estimation. The estimation assumes an almost linear relation between T_g and development rate below the critical molecular weight of PMMA which is estimated to be about M_w~15 kg/mol [2] giving a removal or development rate of about 10 nm/s.

3.3 Glass transition temperature

For simplification, we assumed a discrete layering as depth profile instead of a continuous change of the T_g versus the depth. Figure 7a shows the representative plot of the relative thickness change over temperature for an idealized and theoretical stack of ten layers with the T_g ranging from 30°C to 75°C in these layers. Below the respective T_g the CTE is constant and above as well but with a steeper gradient. Assuming that all layers contribute equally to the film thickness increase gives the summed thickness behavior depicted also in Figure 7a. This summed behavior can be well modelled using the equation derived by *Campbell et al.* [15] for the temperature dependent thickness $h_{(T)}$ of a thin film:

$$h_{(T)} = w\left(\frac{M-G}{2}\right) ln\left(\cosh\left(\frac{T-T_g}{w}\right)\right) + (T-T_g)\left(\frac{M+G}{2}\right) + c \qquad (1)$$

In this equation, w is the width of the glass transition region, M is the CTE of the melt (above T_g), G is the CTE in the glassy region (below T_g), T_g is the glass transition temperature itself and c is the film thickness at T_g. We used a full parameter, least-square fit of the measured data to this equation by Matlab® routines. Figure 7a shows, that the fit result for the summed behavior of the ten-layer stack can exactly describe the theoretical material behavior. For a full depth pro-

file, the thickness of the individual layers would need to be fitted as well using an improved model. However, this is beyond the scope of this contribution and part of ongoing work. However, the model gives already as major output of the fit both the central T_g and the width w of the glass transition region. For the theoretical stack of the ten layers, the determined T_g region was 52.5±22.5 °C. Figure 7b gives the respective derivative and thus CTE for this fitted sum signal. This result is exactly the average of the lowest and the larges T_g in the stack as central T_g and the width being defined by both extreme values. Thus, from the *Campbell* fit so far the largest and the lowest T_g in the complete stack can be extrapolated.

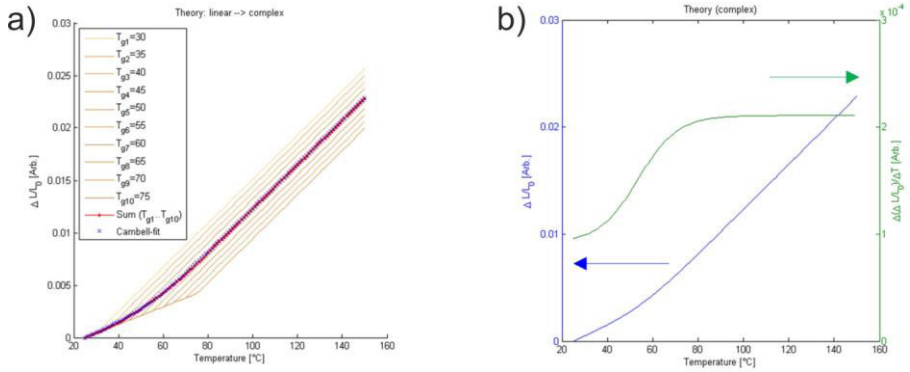

Figure 7. Comparison of a) the summed material behavior of a ten-layer stack with a T_g range from 30°C to 75°C and b) the fitted *Campbell* equation (Eq. (1)) for this material stack together with the derived CTE.

Figure 8 shows the consolidated data points and the least square fit for a 1750 nm thick PMMA120k film after exposure. Two distinct features can be seen in this graph: First, there is a clear T_g region present due to the almost constant thickness change beyond 80°C. Second, the T_g transition region is rather larger and no linear section below a certain lower temperature limit is present. Indeed, the *Campbell* fit gave a T_g region of 49±33 °C with 16° C as lowest and 82°C a largest T_g in this stack. As mentioned above, the model does so far not provide the thickness of the respective regions. However, it confirms that the T_g region extents to room temperature and thus the lower measurable limit of this setup. Considering the very low M_w compounds that have already been removed during the exposure, the very top layers must be just at the limit of volatility under the exposure conditions and thus must have a very low T_g. The upper limit of 82°C is very close to the T_g of about 90-96°C measured for the unexposed PMMA with this setup. This is close to the T_g of 101°C measured by differential scanning calorimetry for the bulk PMMA120k material that is used to prepare the spin-coating solutions. The model is at the moment limited to constant refractive indices which partly explains the difference in the here measured bulk T_g as compared to 122°C measured elsewhere under different conditions [3]. As conclusion, so far a continuous T_g increase from the top towards the substrate is present with very low T_g values of about room temperature at the surface.

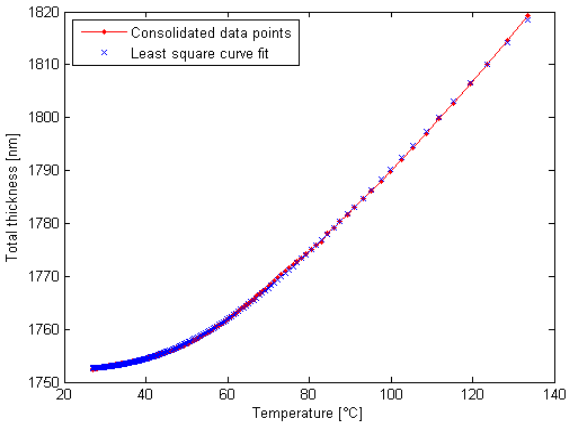

Figure 8. Thickness change of an initially 1750 nm thick PMMA120k film after heating up to 135°C and being measured during the subsequent cooldown.

3.4 Device reflow

Based on the knowledge of this very low T_g top layer, a smoothening of initially very rough surfaces (Fig. 9a,c) into ultra-smooth and optical grade surfaces was achieved (root mean square roughness below 10 nm) (Fig. 9b,d). For this, an intensive exposure for 30 s in a distance of 3 mm was used to enable a significant material modification. The reflow took place at 140°C for 15 min. This post-processing allows a significant time saving during the MPL process. While a rather coarse surface as in Figure 9a,c can be written very fast, a smooth surface similar to Figure 9b,d requires an about ten time longer MPL writing process [11]. Replication into PMMA, post-processing by VUV exposure and global thermal heating as well as the final replication into the product material is mostly still more efficient than the extended writing time. To understand this, one hast to consider that a replication process chain often needs to be established for the high volume manufacturing of micro-optical elements. Once this process chain is in place, the additional steps introduced by our post-processing do not significantly extent the process time and rather save a lot of time during the fabrication of the original patterns used for replication. However, there might be cases that could not effort such a post-processing due to the low volume of fabricated structures and rather use extended direct writing of the required structures.

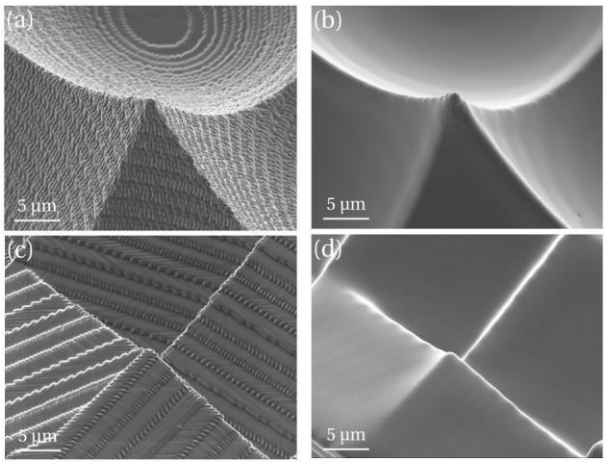

Figure 9. Two optical devices (micro-lens and micro-prism) replicated into PMMA120k from the MPL resist via intermediate molds and subsequently smoothed in a surface confined reflow process and depicted a),c) before and b),d) after reflow.

4. CONCLUSION

We assessed the glass transition temperature distribution in a VUV exposed sample and found that the total modified film thickness might reach down to more than 500 nm but with the most significant region being about the top 300 nm of the exposed PMMA films. In this region, the T_g is extremely reduced almost down to room temperature and this enables a surface selective reflow that does not alter the overall micron-scale shape and rather removes selectively the superficial roughness of micro-optical devices. The achieved material modification fits very well the typical roughness of microfabrication processes. For other processes, the penetration depth can be adjusted with the dose, but this has a direct impact on the T_g contrast, or by using another exposure wavelength with a different penetration characteristic. The presented method is of largest interest for the high volume fabrication of micro-optical devices using polymer replication techniques such as hot embossing, UV-molding or injection molding.

ACKNOWLEDGEMENTS

This project was funded by the Swiss Nanoscience Institute (project A10.13 SurfFlow). The authors express their special thanks to K. Vogelsang (PSI) for support with the hot embossing. The authors also thank M. Rossi (Heptagon) for the support of this project and the useful discussion.

REFERENCES

[1] Dobisz, E.A., Brandow, S.L., Bass, R., and Mitterender, J., "Effects of molecular properties on nanolithography in polymethyl methacrylate," J. Vac. Sci. Technol. B. 18, 107–111 (2000).

[2] Fuchs, K., Friedrich, C., and Weese, J.,"Viscoelastic properties of narrow-distribution poly(methyl methacrylates)," Macromolecules 29, 5893-5901 (1996).

[3] Schleunitz, A., Guzenko, V.A., Messerschmidt, M., Atasoy, H., Kirchner, R., and Schift, H., "Novel 3D micro- and nanofabrication method using thermally activated selective topography equilibration (TASTE) of polymers," Nano Convergence 1:7, 1-8 (2014).

[4] Chidambaram, N, Kirchner, R, Fallica, R., Yu, L., Altana, M. and Schift, H.,"Selective Surface Smoothening of Polymer Microlenses by Depth Confined Softening", Adv. Mater. Technol. 2(5), 1700018 (2017).

[5] Ishihara, Y., and Tanigaki, K., "A high photosensitive IL-CCD image sensor with monolithic resin lens array," Proc. Int. Electron Devices Meeting 29, 497-500 (1983).

[6] Popovic, Z.D., Sprague, R.A., and Connell, G. A. N., "Technique for monolithic fabrication of microlens arrays," Appl. Opt. 27, 1281–1284 (1988).

[7] Kirchner, R., Schleunitz, A., and Schift, H.,"Energy-based thermal reflow simulation for 3D polymer shape prediction using the surface evolver," J. Micromech. Microeng. 24(5), 055010 (7pp) (2014).

[8] Kirchner, R., and Schift, H., "Mobility based 3D simulation of selective, viscoelastic polymer reflow using Surface Evolver," J. Vac. Sci. Technol. 32(6), 06F701 (7pp.) (2014).

[9] Schift, H., Chidambaram, N., Altana. M., and Kirchner, R., "Selective surface smoothening of 3D micro-optical elements", Proc. SPIE 10144, 101440B (2017).

[10] Kirchner, R., Chidambaram, N., Altana, M., and Schift, H., "How post-processing by selective thermal reflow can reduce the roughness of 3D lithography in micro-optical lenses," Proc. SPIE 10095, 1009507 (2017).

[11] Kirchner, R., Chidambaram, N., and Schift, H., "Surface selective VUV and thermal post-processing of thermoplastics for ultra-smooth 3D-printed micro-optics,", submitted to Opt. Eng. (2017).

[12] Kahle, O., Wielsch, U., Metzner, H., Bauer, J., Uhlig, C., and Zawatzki, C., "Temperature and thermal expansion behavior of polymer films investigated by variable temperature spectroscopic ellipsometry," Thin Solid Films 313-314, 803-807 (1998).

[13] Chidambaram, N., Kirchner, R., Altana, M., and Schift, H., "High fidelity 3D thermal nanoimprint with UV curable polydimethyl siloxane stamps," J. Vac. Sci. Technol. B 34(6), 06K401 (2016).

[14] Choi, L.O., Moore, J.A., Corelli, J.C., Silverman, J.P., and Bakhru, H., "Degradation of poly(methylmethacrylate) by deep ultraviolet, x-ray, electron beam, and proton beam irradiations," J. Vac. Sci. Technol. B. 6, 2286-2289 (1988).

[15] Campbell, C. G. and Vogt, B. D., "Examination of the influence of cooperative segmental dynamics on the glass transition and coefficient of thermal expansion in thin films probed using poly(n-alkyl methacrylate)s," Polymer 48/24, 7169-7175 (2007).